Flat Plate Installation Effects on Velocity and Wall Pressure Fields Generated by an Incompressible Jet

Matteo Mancinelli, Alessandro Di Marco, Roberto Camussi
Department of Engineering, University ROMA TRE, Rome, Italy

Summary
The increase of air traffic volume has brought an increasing amount of issues related to carbon and NOx emissions and noise pollution. Aircraft manufacturers are concentrating their efforts to develop technologies to increase aircraft efficiency and consequently to reduce pollutant discharge and noise emission. Ultra High By-Pass Ratio engine concepts provide reduction of fuel consumption and noise emission thanks to a decrease of the jet velocity exhausting from the engine nozzles. In order to keep same thrust, mass flow and therefore section of fan/nacelle diameter should be increased to compensate velocity reduction. Such feature will lead to close-coupled architectures for engine installation under the wing. A strong jet-wing interaction resulting in a change of turbulent mixing in the aeroacoustic field as well as noise enhancement due to reflection phenomena are therefore expected. On the other hand pressure fluctuations on the wing as well as on the fuselage represent the forcing loads which stress panels causing vibrations. Some of these vibrations are re-emitted in the aeroacoustic field as vibration noise, some of them are transmitted in the cockpit as interior noise. In the present work the interaction between a jet and wing or fuselage is reproduced by a flat surface tangential to an incompressible jet at different radial distances from the nozzle axis. The change in the aerodynamic field due to the presence of the rigid plate was studied by hot wire anemometer measurements, which provided a characterization of mean and fluctuating velocity field in the jet plume. Pressure fluctuations acting on the flat plate were studied by cavity-mounted microphones which provided point-wise measurements in stream-wise and span-wise directions. Statistical description of velocity and wall pressure fields are determined in terms of Fourier-domain quantities. Scaling laws for pressure auto-spectra and coherence functions are also presented.

PACS no. 43.28.Ra, 43.50.Nm

1. Introduction

The development of aircraft transportation mainly driven towards improvement of flight efficiency, has brought a strong increase in air traffic volume and issues related to noise emissions and pollutant discharge. High velocity jet exhausting from the engine nozzles is the dominant noise source at take-off and the responsible of pollutant emissions. During cruise, acoustic emissions from the jet are one of the noise sources which contribute to the interior noise. Aircraft manufacturers are concentrating their efforts to develop technologies in order to decrease noise pollution and NOx emissions. UHBPR engine concepts are providing a reduction of jet velocity and a consequent decrease of fuel consumption featuring an increase of fan/nacelle diameter. The reduction of jet velocity is also a benefit for noise abatement, the acoustic intensity being essentially proportional to the eight power of the jet velocity [1]. The increase of nacelle size will lead to close-coupled architecture for under-wing installation of the engine, giving rise to stronger installation effects on jet noise. The jet impact on the surface produces an increase of noise generation which involves a modification of the jet mixing noise source, an enhancement of noise level due to reflection and diffraction phenomena and the appearance of a new noise source named jet-wing or jet-flap interaction noise source. Therefore in order to not jeopardize the break-down of noise due to jet velocity reduction, installation effects have to be mitigated in future aircraft concepts.

On the other hand the pressure fluctuations induced by the jet impinging on the wing and on the fuselage constitute the forcing loads which stress panel structures. The knowledge of wall pressure field is therefore very important to verify structural strength. In the case of the fuselage, the pressure fluctuations acting on the surface cause panels vibrations; some of these vibrations are re-emitted in the aeroacoustic field, some of them are transmitted to the cockpit generating passengers' annoyance.

In the present work the interaction between a jet and an airframe surface was reproduced by the installation of a flat plate close to an incompressible jet. The surface was installed tangentially at different radial distances from the nozzle axis. Hot wire anemometer and microphone measurements were performed in order to characterize the installation effects on velocity and wall pressure fields.

2. Experimental setup and instrumentation

The experiments were carried out in the Laboratory of the Engineering Department of University ROMA TRE. The jet facility reproduces the apparatus developed at the Trinity College of Dublin by [2]. The velocity at the nozzle exhaust varies from $U_{j\,min} = 2\,m/s$ to $U_{j\,MAX} = 50\,m/s$, corresponding to a Reynolds number based on the nozzle diameter spanning from $Re_{min} \approx 10^4$ up to $Re_{MAX} = 1.7*10^5$, which classifies the jet as a moderate Reynolds number jet [3]. The test campaign was carried out at $U_j = 42\,m/s$, to which corresponds a Reynolds number $Re = 1.5 * 10^5$ and a Mach number $M_j \approx 0.12$.

The wooden flat plate was installed tangential to the jet at four radial distances from nozzle axis: $H = 1D, 1.5D, 2D, 2.5D$. The surface was placed on a rigid traverse structure and carefully aligned with the jet flow direction.

The characterization of the installation effects on the mean and fluctuating velocity field was provided by Hot Wire Anemometer (HWA) measurements. The probe was located for different axial distances and was moved along the z-axis, i.e. the direction orthogonal to the surface.

The wall pressure measurements were performed by a cavity-mounted three microphone array. The 1-D spaced pin-holes were properly designed in order to move Helmholtz resonant peaks out of the measured frequency range.

A scheme of the experimental setup described above is shown in figure 1.

3. Experimental results

A preliminary test campaign by hot wire anemometer measurements was carried out in order to characterize the aerodynamic field generated by the facility in the free jet conditions and to verify that the experimental results were in agreement with the ones found in the literature.

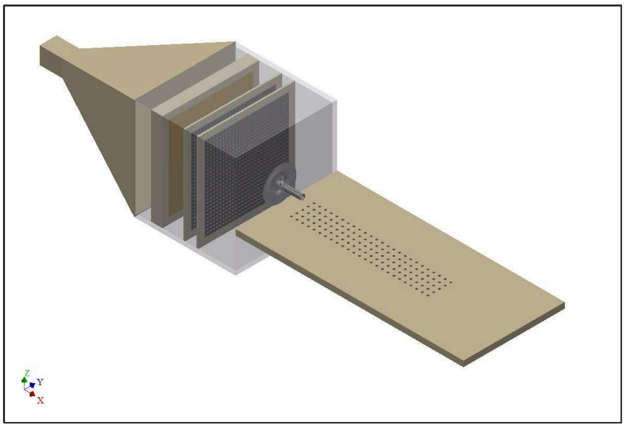

Figure 1. Representation of the jet facility and the experimental setup including the pin-holes distribution on the flat plate and the individuation of the reference system.

The attention was then focused on the installation effects on the aerodynamic field and on the wall pressure field acting on the surface.

3.1. Velocity measurements

The effects on the mean and fluctuating velocity field due to the installation of the flat plate close to the jet were studied for different surface positions from the nozzle axis at different axial distances spanning from $x/D = 1$ to $x/D = 20$. The probe was moved along the z-direction orthogonal to the plate providing velocity and Relative Turbulence Level profiles. Figure 2 shows the mean velocity profiles parametrized in terms of H/D at the axial positions $x/D = 5$, $x/D = 10$, $x/D = 15$, $x/D = 20$. The mean velocity was normalized by the maximum mean velocity measured at each axial distance. It can be observed that the plate affects the axisymmetry of the jet, this effect being dependent on the axial position considered and on the radial position of the plate with respect to the jet.

- For low axial distances the velocity profiles are shifted towards positive z/D coordinates, i.e. in the region opposite to the surface. Such a behaviour is more evident for plate positions closer to the jet.
- As the axial distance increases the velocity profiles start to get close to the surface, the mean velocity maximum being moved to $z/D < 0$. Such a behaviour is faster and sharper for smaller jet-plate separation distances.
- Far downstream in the jet plume the velocity profiles are negative shifted for all the surface radial positions. The jet bends over the surface as a result of the so-called Coanda effect [4].

Figure 3 shows the turbulence intensity profiles along the z-direction for the same axial distances listed above. The velocity standard deviation was normalized by the maximum mean velocity value measured at each axial distance considered. It can be seen

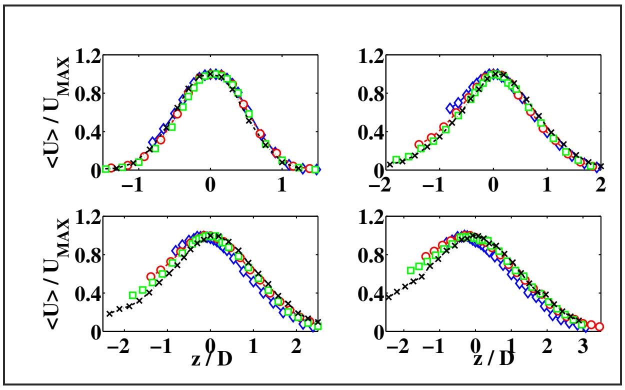

Figure 2. Mean velocity profiles along the z-direction for different jet-plate separation distances H at different axial distances: $x/D = 5$, $x/D = 10$, $x/D = 15$, $x/D = 20$. Blue line corresponds to plate distance $H = 1D$, red line corresponds to $H = 1.5D$, green line corresponds to $H = 2D$, black line corresponds to $H = 2.5D$.

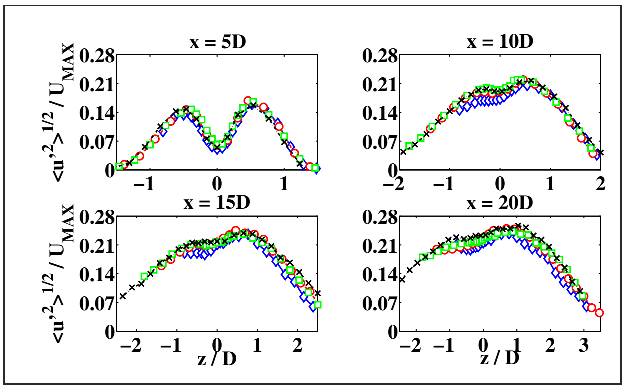

Figure 3. Relative Turbulence Level profiles along the z-direction for different jet-plate separation distances H at different axial distances: $x/D = 5$, $x/D = 10$, $x/D = 15$, $x/D = 20$. Blue line corresponds to plate distance $H = 1D$, red line corresponds to $H = 1.5D$, green line corresponds to $H = 2D$, black line corresponds to $H = 2.5D$.

that the turbulence level is enhanced in the jet region opposite to the surface, while a decrease of the velocity fluctuations can be clearly observed in the region close to the flat plate, this feature being more significant for plate positions closer to the jet. Such a behaviour is in agreement with the results found by [5] in RANS numerical simulations.

3.2. Wall pressure measurements

The wall pressure fluctuations field was measured by a cavity-mounted three microphone array in the streamwise direction from $x/D = 1$ to $x/D = 25$. Pressure transducer measurements were also performed to characterize the mean pressure field.

Figure 4 shows the axial evolution of the Sound Pressure Spectrum Level ($SPSL$) along the jet axis for all the jet-plate separation distances at a fixed axial position: $x/D = 1$, $x/D = 5$, $x/D = 10$, $x/D = 15$, $x/D = 20$, $x/D = 25$. According to [6], the $SPSL$ was calculated as follows:

$$SPSL = 10 \log_{10} \frac{PSD\,\Delta f_{ref}}{p_{ref}^2} \tag{1}$$

where PSD is the Power Spectral Density, while $\Delta f_{ref} = 1\,Hz$ and $p_{ref} = 20\,\mu Pa$ are respectively the reference frequency and the reference pressure. The energy content and the spectral shape is strongly dependent on the radial distance of the plate from the jet and on the axial distance considered. Such a behaviour is clearly evident at low axial distances for which the spectra amplitude is much higher for lower H, while for larger surface radial distances the energy is much lower and peaks due to background noise emerge. As the axial distance increases the energy rises and the spectral shape changes accordingly covering the whole frequency range. Such a behaviour is due to the relationship between the jet-surface separation distance and the axial distance for which the jet has impacted on the surface, the energy of wall pressure fluctuations being much higher after the jet impingement on the plate. Indeed the wall pressure energy is significantly different if the jet impact over the surface occurs in the potential core region, in the transition region or in the developed region. Further downstream the impact position a quasi-equilibrium Turbulent Boundary Layer (TBL) can be established due to the development of the flow over the surface. Such inference is further supported by the decay laws typical of wall pressure fluctuations in TBLs found in the spectra corresponding to high axial distances [7]. A slope $\propto St_D^{-1}$ related to the energy decay in the overlap region is found in the frequency range after the spectrum peak; in the mid-frequency range an energy decay of $-7/3$ typical of turbulent flows is clearly observed, while at high frequencies the dominant viscous effects determine a power decay law St_D^{-5}.

The axial evolution of the mean pressure coefficient and the root mean square pressure coefficient is shown respectively in figure 5 and in figure 6. The pressure coefficients are defined as follows [8]:

$$c_p = \frac{< p > - p_\infty}{1/2 \rho U_j^2} \tag{2}$$

$$c_{p_{RMS}} = \frac{p_{RMS}}{1/2 \rho U_j^2} \tag{3}$$

Three different regions of jet-surface interaction were determined based on the trend along the jet axis of the pressure coefficients defined in (2) and (3).

- First region: the mean pressure remains almost constant while the $c_{p_{RMS}}$ increases.
- Second region: the mean pressure rises reaching its maximum value while the root mean square pressure remains almost constant.

Table I. Resume of the individuation of the jet-surface interaction regions

	Plate distance	Axial position
End of region 1	$H = 1D$	$x/D = 3$
	$H = 1.5D$	$x/D = 6$
	$H = 2D$	$x/D = 9$
	$H = 2.5D$	$x/D = 12$
End of region 2	$H = 1D$	$x/D = 9$
	$H = 1.5D$	$x/D = 13$
	$H = 2D$	$x/D = 13$
	$H = 2.5D$	?

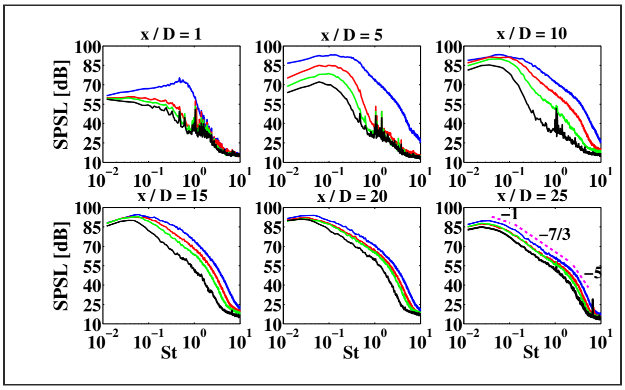

Figure 4. Sound Pressure Spectrum Level of wall pressure fluctuations along the jet axis at different axial distances for different plate distances from the jet: blue line corresponds to plate distance $H = 1D$, red line corresponds to $H = 1.5D$, green line corresponds to $H = 2D$, black line corresponds to $H = 2.5D$.

- Third region: both the c_p and the $c_{p_{RMS}}$ decrease, the first one recovering its initial amplitude, the second one being larger as a result of the development of a turbulent boundary layer.

The individuation of the different regions of jet-surface interaction for all the plate radial distances from the jet is resumed in table I. It has to be pointed out that the beginning of the region 2 corresponds to the axial position of the jet impact over the plate. Such inference was also demonstrated computing the free-jet aperture angle by HWA measurements. Moreover for the $H = 2.5D$ configuration the distinction between the second and the third region is not clearly detectable. This behaviour is due to the fact that the jet impinges on the plate very far from the nozzle exhaust, its mean kinetic energy being much lower as well as its pressure signature on the plate.

3.2.1. Spectral modeling

With respect to the determination of the jet-plate interaction regions described above, a scaling criterion for pressure auto-spectra belonging to the same region

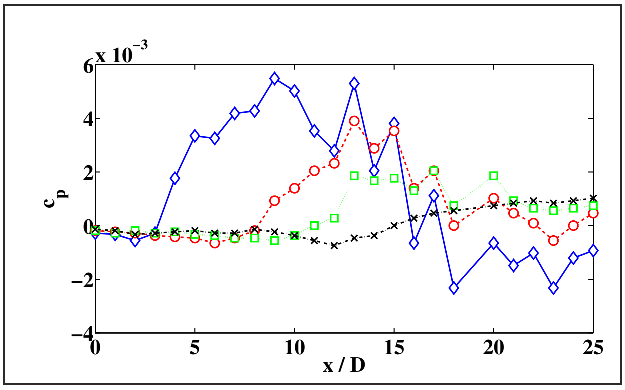

Figure 5. Axial evolution of the mean pressure coefficient along the jet axis for different flat plate radial positions from the jet. Blue line corresponds to $H = 1D$, red line corresponds to $H = 1.5D$, green line corresponds to $H = 2D$, black line corresponds to $H = 2.5D$

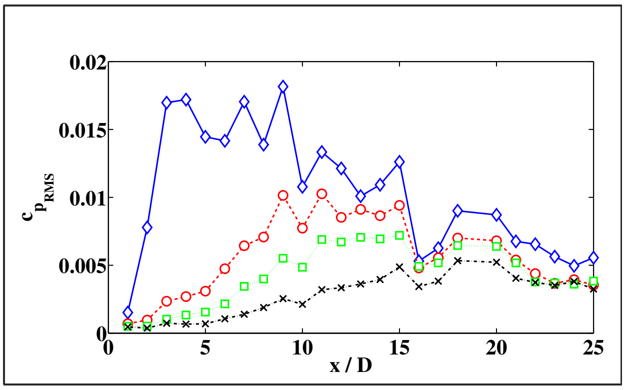

Figure 6. Axial evolution of the root mean square pressure coefficient along the jet axis for different flat plate radial positions from the jet. Blue line corresponds to $H = 1D$, red line corresponds to $H = 1.5D$, green line corresponds to $H = 2D$, black line corresponds to $H = 2.5D$

based on outer aerodynamic variables and main geometrical length-scales was derived. Pressure spectra were normalized by the dynamic pressure related to the convection velocity U_c, while the reference time-scale was estimated as the time occurring to a fluid particle convected by the mean flow to reach the surface: H/U_c. The convection velocity was calculated from the time-delay of the cross-correlation peak between two consecutive microphone signals. The spectra were plotted against a Strouhal number based on the plate distance from the jet H and the jet velocity at the nozzle exhaust U_j. The variables just defined are following resumed:

$$PSD_{scaled} = \frac{PSD}{(0.5\rho U_c^2)^2 \dfrac{H}{U_c}} \tag{4}$$

$$St_H = \frac{f\,H}{U_j} \tag{5}$$

The scaling criterion applies to spectra at different axial locations and different jet-plate separation distances belonging to the same jet-surface interaction region for an axial distance far enough from the nozzle exhaust so that the jet had already impacted over the surface. Figure 7 shows the scaled PSDs for wall pressure signals belonging to region 2 and region 3. The collapse of the spectra was well verified, such result suggesting that the wall pressure spectra behaviour for the jet-surface interaction becomes universal before a TBL condition is reached.

The behaviour of the wall pressure field was further analyzed by computing the coherence function for the same axial distances for which the pressure spectra collapse was verified. The coherence function is defined as follows [9]:

$$\gamma(\xi,\omega) = \frac{|\Phi_{p_i p_j}(\xi,\omega)|}{\left[\Phi_{p_i}(\omega)\,\Phi_{p_j}(\omega)\right]^{1/2}} \tag{6}$$

where $\Phi_{p_i p_j}$ is the cross-spectrum, Φ_{p_i} and Φ_{p_j} are the auto-spectra of two consecutive microphones, ω is the angular frequency and ξ is the separation distance between two consecutive microphones. In the present work $\xi = 1D$. The experimental results were compared with the analytical Corcos' model for wall pressure fluctuations in turbulent boundary layers [10]:

$$\gamma(\xi,\omega) = exp\left(-\alpha\frac{\omega\,\xi}{U_c}\right) \tag{7}$$

The value of the coefficient α was determined by a least mean square optimization from the experimental data. Figure 8 shows the experimental coherence functions parametrized in terms of H/D at given axial locations and the comparison with the predictions given by Corcos' formulation. The exponential trend of the Corcos' model is reproduced by the experimental data, although for small axial distances a steeper decay along the normalized angular frequency is found for larger H. As the axial distance increases and a developed TBL approaches, the experimental data become less scattered and the values of the Corcos' model coefficient are comparable with the ones found in the literature for all the jet-plate radial distances. Such a behaviour is better highlighted in figure 9 in which the axial evolution of the modulus of the Corcos' model coefficient derived from the experiments is shown for all H. Values ranging from 0.1 to 0.19 found in the literature ([11]) are also reported. As it can be seen for the smallest H the experimental values of the Corcos' model coefficient are included in the range provided in the literature for all the axial locations considered. For larger H at low axial distances the coefficient values are higher than the ones given by Corcos. As the axial distance increases $|\alpha|$ decreases and the tendency is to reproduce the amplitude of the Corcos' formulation, such a behaviour being a proof that a turbulent boundary layer is approaching.

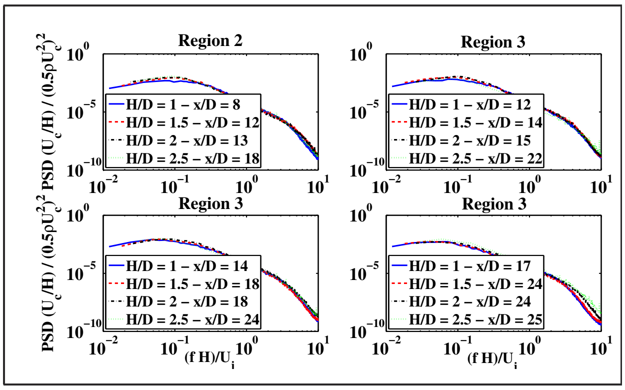

Figure 7. Scaled pressure spectra for different plate radial distances and different axial locations belonging to the same jet-surface interaction region. Blue line corresponds to $H = 1D$, red line corresponds to $H = 1.5D$, green line corresponds to $H = 2D$, black line corresponds to $H = 2.5D$

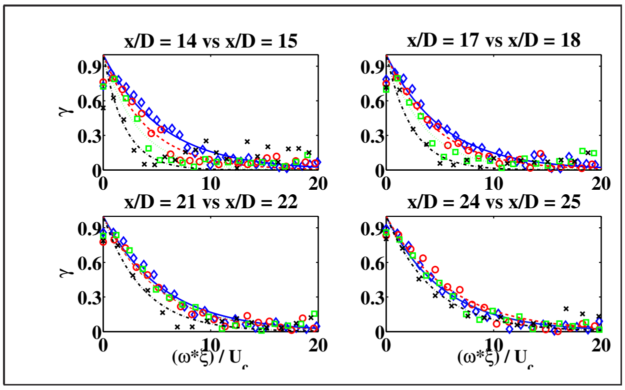

Figure 8. Coherence functions for different axial distances along the jet axis: markers are related to experimental data, lines are referred to Corcos' model formulation. Blue color corresponds to $H = 1D$, red color corresponds to $H = 1.5D$, green color corresponds to $H = 2D$, black color corresponds to $H = 2.5D$

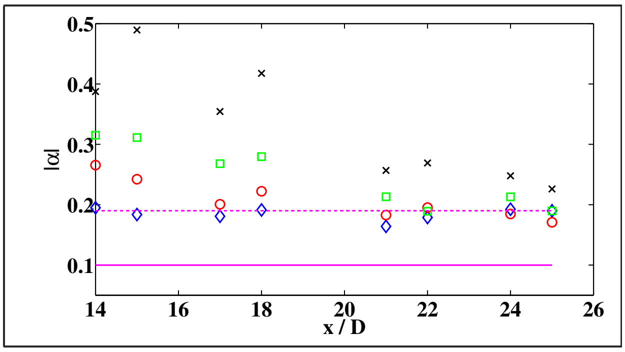

Figure 9. Axial variation of the experimental Corcos' model coefficients along the jet axis for different jet-plate separation distances: blue $\diamond$ correspond to $H = 1D$, red $\circ$ correspond to $H = 1.5D$, green $\boxdot$ correspond to $H = 2D$, black $\times$ correspond to $H = 2.5D$. Solid and dashed line correspond respectively to the lower and upper limit of Corcos' model coefficients found in the literature.

4. Conclusions

In the present work the interaction between an incompressible moderate Reynolds number jet and a tangential flat plate was analyzed. The study was performed by an extensive experimental test campaign which involved velocity and wall pressure measurements for different surface radial distances from the nozzle axis. The velocity measurements were performed by hot wire anemometer providing the effects on the mean and fluctuating aerodynamic field due to the plate installation. The wall pressure measurements were performed by a pressure transducer and by cavity-mounted microphone array providing respectively the mean and fluctuating wall pressure field over the surface.

The plate installation tangentially to the jet affects both the mean and the fluctuating velocity field, the effect being dependent on the radial separation distance. For low axial distances the mean velocity profiles are shifted towards the region opposite to the plate; as the axial distance increases the velocity profiles are moved in the jet region close to the surface. The jet axis, i.e. the z-location for which the mean velocity value has a maximum, no longer coincides with the nozzle axis. Further downstream the jet bends over the surface as a result of the Coanda effect. For what concerns the fluctuating velocity field, the turbulence profiles are shifted in the jet region opposite to the plate, while the velocity fluctuations intensity is lowered in the region close to the surface. The plate has the effect to break-down the larger turbulent structures in the jet. Such inference was further demonstrated by the trend of the cross-correlation between the wall pressure signals. For more details the reader can refer to [12].

The analysis of the wall pressure fluctuations spectra showed that the energy content and the spectral shape change significantly along the stream-wise direction. Moreover for a given axial location, the amplitude and the shape of the spectra is strongly dependent on the jet-plate separation distance. Such a behaviour is related to the different axial position for which the jet impacts on the surface for the different plate radial distances from the jet, the energy of the pressure fluctuations being much higher after the jet impingement over the surface. Further downstream the pressure spectra show the typical energy decay laws of wall pressure fluctuations in TBLs. Three regions of jet-surface interaction were detected based on the axial evolution of the mean pressure coefficient and the root mean square pressure coefficient. A scaling criterion for pressure auto-spectra based on outer aerodynamic variables and main geometrical length-scales was derived for spectra belonging to the same region of jet-surface interaction. The collapse was satisfactory. The analysis of the coherence function showed that the exponential decay of the Corcos' model for wall pressure fluctuations in TBLs is reproduced by the experimental data. For the closest plate position the experimental Corcos coefficients are included in the range found in the literature for all the axial locations considered. For larger H at low axial distances the coefficient values are higher than the analytical ones; as the axial distance increases the amplitude decreases reproducing the values provided by Corcos' formulation. Such a behaviour being a proof that far downstream the wall pressure fluctuations related to the jet-surface interaction approach the physics of a quasi-equilibrium turbulent boundary layer.

Acknowledgement

The authors acknowledge the support of the EU collaborative project JERONIMO (ACP2-GA-2012-314692), funded under the 7th Framework Program.

References

[1] M. J. Lighthill: On Sound Generated Aerodynamically I. General Theory. Proc. R. Soc. Lond. 1952, 564-587.

[2] L. Chatellier, J. Fitzpatrick: Spatio-temporal Correlation Analysis of Turbulent Flows Using Global and Single-point Measurements. Experiments in Fluids 38 (2005) 563-575.

[3] C. Bogey, O. Marsden, C. Bailly: Effects of Moderate Reynolds Numbers on Subsonic Round Jets with Highly Disturbed Nozzle-exit Boundary Layers. Physics of Fluids 24 (2012) 105107.

[4] B. Launder, W. Rodi: The Turbulent Wall Jet Measurements and Modeling. Annual Review of Fluid Mechanics 15 (1983) 429-459.

[5] M. J. Smith, S. A. E. Miller: The Effects of Surfaces on the Aerodynamics and Acoustics of Jet Flows. AIAA 2013, 2013-2041.

[6] A. D. Pierce: Acoustics: An Introduction To Its Physical Principles and Applications. Acoustical Society of America, New York, 1989.

[7] Y. Hwang, W. K. Bonness, S. A. Hambric: Comparison of Semi-empirical Models for Turbulent Boundary Layer Wall Pressure Spectra. Journal of Sound and Vibration 319 (2009) 199-217.

[8] R. Camussi, M. Felli, F. Pereira, G. Aloisio, A. Di Marco: Statistical Properties of Wall Pressure Fluctuations Over a Forward-facing Step. Physics of Fluids 20 (2008) 075113.

[9] A. Di Marco, R. Camussi, M. Bernardini, S. Pirozzoli: Wall Pressure Coherence in Supersonic Turbulent Boundary Layers. Journal of Fluid Mechanics 732 (2013) 445-456.

[10] T. M. Farabee, M. J. Casarella: Spectral Features of Wall Pressure Fluctuations Beneath Turbulent Boundary Layers. Physics of Fluids 3 (1991) 2410-2420.

[11] T. F. Brooks, T. H. Hodgson: Trailing Edge Noise Prediction from Measured Surface Pressures. Journal of Sound and Vibration 78 (1981) 69-117.

[12] A. Di Marco, M. Mancinelli, R. Camussi: Pressure and Velocity Measurements of an Incompressible Moderate Reynolds Number Jet Interacting with a Tangential Flat Plate. Journal of Fluid Mechanics. Under review